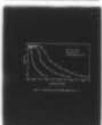TEXAS INST FOR COMPUTATIONAL MECHANICS AUSTIN
ADAPTIVE REFINEMENT AND NONLINEAR FLUID PROBLEMS.(U)
MAY 79 G F CAREY

UNCLASSIFIED   TICOM-79-3

NL

| OF |
AD
A069830

END
DATE
FILMED

7--79

DDC

1.0

1.1

1.25

4.5
5.0
5.6

2.8

3.2

3.6

4.0

2.5

2.2

2.0

1.8

1.4

1.6

MICROCOPY RESOLUTION TEST CHART
NATIONAL BUREAU OF STANDARDS-1963-A

LEVEL

DA069830

ADAPTIVE REFINEMENT AND NONLINEAR FLUID PROBLEMS

by

Graham F. Carey

TICOM Report #79 - 3

May 1979
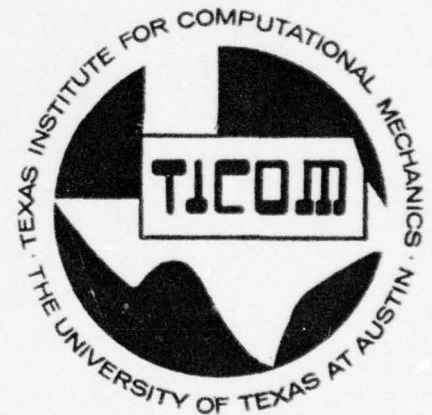
THE TEXAS INSTITUTE *for* COMPUTATIONAL MECHANICS

THE UNIVERSITY OF TEXAS AT AUSTIN

79 06 12 157

TECHNICAL REPORT, TR-1

ADAPTIVE REFINEMENT AND NONLINEAR FLUID PROBLEMS*

Graham F. Carey

Texas Institute for Computational Mechanics
University of Texas at Austin, U.S.A.

May 79   44 p.

TICOM-79-3, TR-1

DDC
RECEIVED
JUN 13 1979
C

408 958

TABLE OF CONTENTS

Page

ADAPTIVE REFINEMENT AND NONLINEAR FLUID PROBLEMS *

Graham F. Carey

Texas Institute for Computational Mechanics
University of Texas at Austin, U.S.A.

Summary

Two principal and related topics are considered: (1) adaptive mesh refinement for finite element computations, and (2) mesh refinement specifically for nonlinear flow problems. In the first instance the residual and associated trace theorems for variational problems are introduced to relate the solution error to a computable residual. This provides a theoretical basis for a mesh refinement strategy.

A corresponding adaptive refinement procedure that automatically and selectively refines the mesh is formulated and implemented for a class of nonlinear transport problems in chemical engineering. In particular, a nonlinear problem with a boundary-layer solution is investigated. The strategy of interweaving Newton solution and mesh refinement proves particularly efficient.

Two-dimensional compressible and transonic flows are next examined. Mesh refinement of subregions of the flow field is applied to yield high solution near a singularity for both the linear and nonlinear flows. Refinement and Newton iteration are combined, together with Mach number parameterization, to determine an efficient and accurate solution algorithm. Similar points for nonlienar viscous problems are also reviewed.

---

i

ADAPTIVE REFINEMENT AND NONLINEAR FLUID PROBLEMS

Texas Institute for Computational Mechanics
University of Texas at Austin, U.S.A.

1. Introduction

In approximating the solution of boundary-value problems by finite
element methods, we are continually confronted with the problem of deciding
on a mesh, assessing the quality of the solution obtained with that mesh,
and perhaps iteratively adjusting and enriching the mesh. As the solution
and its derivatives may vary markedly over the domain, nonuniform meshes
are warranted in the interests of computational efficiency. This is es-
pecially true of nonlinear problems where solutions exhibit layer or singu-
lar behavior.

Of course, this refinement problem applies quite generally to discrete
methods for boundary-value problems. In the present article we shall confine
the choice of applications to flow problems. Fluid mechanics has long been
a rich source of problems in applied mathematics. Many classical methods
of analysis, such as analytic function theory, have their origins and motiva-
tion in fluid mechanics. Problems with singularities, interior layers, boun-
dary layers and nonlinearities, where meshes are important, are commonplace.
This is true of the entire gamut of viscous, compressible, rotational and
other flows and also of transport problems which are included here.

The focus of this article is the underlying mathematical analysis, fi-
nite element technique, algorithms and implementation of mesh refinement in
this context. Special points of interest concerning refinement in layers
and near singularities , and solution strategies, are developed for representa-
tive steady flow problems. Throughout, important points are demonstrated using

1

select problems drawn primarily from ongoing research studies of this topic. Similar investigations have also been carried out for nonlinear problems in solid mechanics and work in both areas is continuing. Where appropriate, other research activities related to this topic are also indicated.

2. Refinement and Residuals

In many engineering applications one is able to predict those subregions where the solution is changing markedly and use a finer mesh there. For instance, the form of the loading or boundary data and shape of the domain may indicate where the mesh needs to be fine. A preliminary computation on a coarse uniform mesh may also be useful. Yet these actions only alleviate the situation and do not resolve the main problem - the degree of local subdivision is still unknown.

Ideally, we require an algorithm which selectively refines the mesh in appropriate subregions of the domain. This implies that we have some criterion for automatically assessing the quality of the approximate solution on intermediate finite element meshes. It is easy to devise *ad hoc* principles for refining the mesh. Monitoring the changes in local solution behavior between successive meshes and extrapolating to the next mesh is perhaps the simplest strategy and will often work reasonably well. We also note that one can readily concoct pathological examples such as highly oscillatory functions that will defy any refinement procedure (Try $u = \frac{1}{\varepsilon} \sin \varepsilon x$, $0 < \varepsilon \ll 1$).

A criterion which has a more rigorous foundation in the approximate method itself is more desirable. Finite element methods are often based on energy principles: the energy functional is minimized for the exact solution, and the approximate solution minimizes the same functional over a finite

dimensional subspace S(M), the class of finite element approximations on a given mesh M . Refining the mesh produces a broader class of functions and a lower value to the approximate global energy. This suggests that computation of the energy for successive meshes will indicate the global quality of the solution and meshes. Perhaps one can extend this argument to the local accuracy of the energy contribution from individual elements or groups of elements as they are refined.

What may we infer regarding those problems where a classical energy principle is not available? The weak variational statement and generalized solution constitute an equivalent integral formulation of a boundary-value problem. The classical minimization principles are then included as a special category. In turn, we recognize that the variational problem can be interpreted as a particular form of the method of weighted residuals. We now appeal to this characterization to establish a suitable refinement criterion. For a given approximation, the residual represents the amount by which the differential equation fails to be satisfied. An exact classical solution yields residual $R \equiv 0$. The variational problem is constructed from a duality pairing between the residual $R(u)$ and test functions v .

The various approximation methods require that the residual be close to zero, in some sense. That is, the projection of the residual in the test space is zero. For example: in collocation the test functions are delta functions and the residual is forced to be zero at specific points; in Galerkin methods the projection of the residual in the approximation space or a subspace is zero - in an appropriate norm, a point we shall shortly develop. This leads us to explore the use of the residual as an indication of solution accuracy globally in the domain and perhaps even locally. Except for very simple bases, the residual will usually be non-zero and well defined on an element and the norms of the residual easily

calculated there. For example, we could write for element Ω_e the usual L_2 norm

$$\| R \|_{\Omega_e} = \left\{ \int_{\Omega_e} R^2 \, d\Omega \right\}^{\frac{1}{2}} \tag{1}$$

Then a refinement scheme might be introduced that refines those elements where $\| R \|_{\Omega_e}$ per unit volume is large. The simplest case, a piecewise linear element draws our attention to a difficulty here. The second order derivatives u" will not contribute to the residual in the element interior but rather as boundary terms (jumps) at the element interfaces. These should be included in the residual evaluation of equation (1).

The foregoing discussion motivates a residual analysis to provide the desired refinement criterion. In principle, we seek global and local error bounds for the solution in terms of *computable* element residuals. We shall develop this basic analysis for the standard two-point problem. The trace theorems allow us to employ the same residual analysis in higher dimensions [1].

Following this theoretical analysis, residuals are employed in adaptive refinement and related procedures. A particular point we shall examine is that of interweaving adaptive mesh refinement with nonlinear solution iteration. Numerical experiments are conducted to confirm that this is computationally very effective. The particular examples described concern nonlinear heat and mass transport with a boundary layer solution and compressible flow problems.

3. One-Dimensional Analysis

The one-dimensional problem has a very special connectivity - adjacent elements meet at their end nodes. Since we are considering mesh refinement strategies here, this implies that refinement by multiple "splittings" of elements is relatively straightforward. New nodal points are introduced and the continuity and differentiability of the approximation ($C^0, C^1, \ldots$ functions)

are readily maintained.

We first summarize some fundamental properties of the residual for linear two-point problems. The details of the proofs are described elsewhere [2-4]. Consider the standard linear problem,

$$-(p(x)u')' + q(x)u = f(x) \quad \text{in} \quad \Omega = (0,1) \tag{2}$$

with $u(0) = u(1) = 0$.

A generalized (weak) solution to equation (2) can be determined among admissible functions $u(x) \in H_0^1(\Omega)$ by requiring that

$$\int_0^1 pu'v' \, dx + \int_0^1 quv \, dx - \int_0^1 fv \, dx = 0 \tag{3}$$

for all $v(x) \in H_0^1(\Omega)$.

Let L denote the linear differential operator in equation (2). Then, for an approximate solution $U(x) \in H_0^1(\Omega)$ the residual $R(x) = LU - f$ is defined in a distributional sense by equation (3). Since $Lu = f$ and $LU = R + f$, then $L(U - u) = R$ or $L\varepsilon = R$ where $\varepsilon = U - u$ is the solution error. Now as u and U are in H_0^1, so is ε, and R is in the dual space $(H_0^1)' = H^{-1}$. From Hilbert Space Theory, the induced norm in H^{-1} is

$$\| R \|_{-1,\Omega} = \sup_{\substack{w \in H_0^1 \\ w \neq 0}} \frac{|\langle R,w \rangle|}{\| w \|_{1,\Omega}} \tag{4}$$

Since $L\varepsilon = R$ with $L\varepsilon = -(p\varepsilon')' + q\varepsilon$, then from (3) we have on setting $v = \varepsilon$ and simplifying

$$\| \varepsilon \|_{1,\Omega} \leq C \| R \|_{-1,\Omega} \tag{5}$$

where C is a constant.

This basic inequality forms the starting point of our residual analysis. The H^{-1}-norm is not readily computed, so we seek to replace the bound by an expression involving computable element residuals. To evaluate $\| R \|_{-1}$, we return to the definition of equation (4) and examine the duality pairing. On a partition of n elements of C^0-Lagrange type,

$$\langle R,w \rangle \;\; = \;\; \sum_{i=1}^{n} \int_{\Omega_i} (pu'w' + quw - fw)dx \tag{6}$$

Integrate by parts on the entire domain as a union of elements to obtain

$$\langle R,w \rangle = \sum_{i=1}^{n} \left[\int_{\Omega_i} \{-(pu')' + qu - f\}w \, dx + \int_{\Omega_i} (pu'w)' \, dx \right] \tag{7}$$

Taking absolute values and applying the Cauchy-Schwarz inequality to each integral, we obtain

$$| \langle R,w \rangle | \leq \sum_{i=1}^{n} \{ \| R \|_{0,\Omega_i} \| w \|_{0,\Omega_i} + h_i^{-\frac{1}{2}} \, |[pu'(x_{i+1}) - pu'(x_i)]| \| w \|_{1,\Omega_i} \tag{8}$$

Since $\| w \|_0 \leq \| w \|_1$,

$$| \langle R,w \rangle | \leq \sum_{i=1}^{n} \{ \| R \|_{0,\Omega_i} + h_i^{-\frac{1}{2}} |pu'(x_{i+1}) - pu'(x_i)| \} \| w \|_{1,\Omega_i} \tag{9}$$

From the Schwarz and Hölder inequalities for finite sums,

$$| \langle R,w \rangle | \leq \left(\sum_{i=1}^{n} \{ \| R \|_{0,\Omega_i} + h_i^{-\frac{1}{2}} (|pu'(x_{i+1}) - pu'(x_i)|) \}^2 \right)^{\frac{1}{2}} \left(\sum_{i=1}^{n} \| w \|_{1,\Omega_i}^2 \right)^{\frac{1}{2}} \tag{10}$$

We define the specific element residual as

$$\||| R \||| _i = \{ \| R \|_{0,\Omega_i} + h_i^{-\frac{1}{2}}(|pu'(x_{i+1}) - pu'(x_i)|)\} \tag{11}$$

so that

$$| \langle R,w \rangle | \leq \{ \sum_{i=1}^{n} \||| R \||| _i^2 \}^{\frac{1}{2}} \| w \|_{1,\Omega} \tag{12}$$

Using this in equations (4.4),

$$\| R \|_{-1} \leq \left(\sum_{i=1}^{n} \||| R \||| _i^2 \right)^{\frac{1}{2}} = \||| R \||| _\Omega \tag{13}$$

and inequality (4.9) is replaced by the global residual bound

$$\| \varepsilon \|_{1,\Omega} \leq C \||| R \||| _\Omega \tag{14}$$

The element contribution to $\||| R \||| _\Omega$ may be computed, within a constant C, from equation (13). Since C is independent of h_i and w, the inequality (14) is a practical bound that can be utilized directly in our refinement criterion. As $\||| R \||| _i$ is reduced by refinement, $\||| R \||| _\Omega$ will also decrease as will the global error $\| \varepsilon \|_{1,\Omega}$.

To obtain an effective local refinement criterion we need a local bound on an element of the same form as inequality (14). Consider a subsidiary problem posed on an element and with nonhomogeneous boundary data (approximations to the solution values) at the element end nodes. By similar arguments to the above we obtain the local error bound

$$\| \varepsilon \|_{1,\Omega_e} \leq C \||| R \||| _{\Omega_e} + \| \eta \|_{1,\Omega_e} \tag{15}$$

where η arises from the nonhomogeneous data and satisfies $L\eta = 0$ in Ω_e, $\eta = \varepsilon$ at the end nodes of an element. Using the trace theorems and maximum

principles, $\| \eta \|_{1,\Omega_e}$ is negligible for $h = \max\limits_{i} h_i$ sufficiently small and Ω_e not near the boundary of Ω. Hence, inequality (14) provides the desired local bound.

4. Algorithm

This residual analysis establishes a theoretical basis for developing an adaptive refinement strategy for two-point problems. We now utilize this residual criterion in a statistical procedure in which subregions are located and refined automatically as part of the algorithm. The statistical approach is quite robust as we demonstrate in numerical experiments.

Consider an initial mesh $M_0(\Omega)$. A finite element approximation $U(x)$ is computed on $M_0(\Omega)$ and the element residuals computed according to equation (11). The mean $\bar{R}(M_0)$ and standard deviation $s(M_0)$ are calculated for the set of element residuals $\{\|\|R\|\|_i\}$. We define refinement "intervals" on the distribution of element residuals by considering the intervals $I_1 = (-\infty, \bar{R} + ks)$, $I_2 = (\bar{R} + ks, \bar{R} + 2ks), \ldots, I_t = (\bar{R} + (t-1)ks, \infty)$, where k represents the fraction of a standard deviation in each interval. For example, if $k = 1$ the refinement intervals lie $1,2,3,\ldots,t$ standard deviations above the mean residual. Now if $\|\|R\|\|_i$ is located in refinement interval j, then element i is refined to j elements. An estimate of the solution at the newly-introduced nodes is provided by local interpolation in the old basis. On completion of the refinement of $M_0(\Omega)$ to $M_1(\Omega)$ a solution can be computed on $M_1(\Omega)$.

The residual calculations are straightforward and readily implemented in a computer program. In the algorithm above we begin with an initial coarse mesh $M_0(\Omega)$ and the algorithm selectively refines the mesh in a systematic manner to the final mesh $M_f(\Omega)$ with solution $u(x; M_f(\Omega))$.

It is not important that the criterion be precise at each mesh iteration.

Rather, the sequence of meshes generated need only approach an appropriate final configuration. The means $\{\overline{R}\}$ of successive residual distributions regress towards zero and a natural gradation of the mesh is inherent in the scheme. These points are demonstrated in the example below.

5. Example: Interior-Layer Problem

Consider the two-point problem

$$-[\{\frac{1}{\alpha} + \alpha(x - \overline{x})^2\}u']' = 2[1 + \alpha(x - \overline{x})\tan^{-1}\alpha(x - \overline{x}) + \tan^{-1}\alpha\overline{x}] \quad (16)$$

in $0 < x < 1$ with $u(0) = u(1) = 0$. If α is large, say $(O(10^2))$, then the solution

$$u(x) = (1 - x)[\tan^{-1}\alpha(x - \overline{x}) + \tan^{-1}\alpha\overline{x}] \quad (17)$$

has an interior layer in the neighborhood of $x = \overline{x}$.

Numerical results are presented here for $\alpha = 100$ and $\overline{x} = .36388$. In the numerical experiment C^0 quartic elements are used, beginning with an initial mesh $M_0(\Omega)$ of four equal elements. After 8 adaptive refinements, the finite element mesh consists of 29 elements with a gradual transition from either side to smaller elements within the layer [7 in (0,.25); 4 in (.25,.325); 9 in (.325,.375); 4 in (.375,.425); 5 in (.425,1.0)]. At this mesh level the global residual is 7.479. On subsequent refinements many elements are located in the interval (0.25,0.5), particularly at the interior layer. On the "final" mesh of 74 elements (43 of them in [.3125,.4375]) the global residual is .812. The H^1 and H^0 norms of the global solution error are 9.895×10^{-3} and 1.411×10^{-4}, respectively.

It is instructive to compare global residual and errors for the entire refinement history. In Figure 1 we present typical results as a log-log plot of global residual $\||R\||$ versus H^0 and H^1 norms of the solution error. The

straight line corresponds to a linear regression of these results. The residual and error decrease monotonically on successive refinements and the experimental values are consistent with earlier theoretical results. Empirically, we have for this example, $\| \varepsilon \|_0 = 4.703 \times 10^{-6} \||R\||^{1.706}$ and $\| \varepsilon \|_1 = 2.212 \times 10^{-3} \||R\||^{1.517}$. The H^1 error norm (slope 0.66) decreases more slowly than the H^0 error norm (slope 0.59). Qualitatively, this resembles the theoretical result for uniform mesh refinement. Data points for a uniform mesh refinement are also plotted and lie on the linear regression curves in the figure. This confirms the argument that the ability to compute on an adaptive non-uniform grid using the residual criterion essentially enables one to progress down the straight lines rapidly, reducing the error in the solution while incurring low storage and computation penalties.

[Figure 1]

6. Nonlinear Problems

When nonlinear problems are considered, automated mesh refinement is even more appealing, particularly if the solutions are not very smooth or if layers again occur. Nonlinear analysis is a difficult topic and some of the points of particular concern in finite element analysis of nonlinear boundary-value problems are related to non-uniqueness and convergence. Here we wish to examine the benefits of interweaving iterative solution and adaptive mesh refinement. The finite element problem on each grid now requires the solution of a nonlinear system of algebraic equations. Evidently, it should be more efficient to refine the mesh as soon as the solution iterate on a given mesh has assumed the approximate form of a converged solution, rather than compute a fully-converged solution on an inadequate grid prior to refinement. This implies that one must estimate when to cease iteration and refine the current

grid. The relative and absolute changes of element residuals may be used to determine a stopping criterion.

To explore this strategy, we consider a class of nonlinear problems arising in heat and mass flow in chemical engineering. The design of effective catalytic reactors, involving impregnated porous catalyst in the solid phase immersed in fluid reactants, requires an understanding of the transport processes in the solid material. Consider the diffusion of heat and mass in a catalyst pellet where chemical reaction takes place. These problems are characterized by nonlinear reaction rate terms, often involving exponentials, and will exhibit multiple solution states and interior-layer or boundary-layer behavior for some ranges of the reaction rate parameters.

Chemical engineers have developed high-order global approximation methods to solve these "effectiveness factor" problems very accurately [5]. However, these global methods prove unsatisfactory for the more difficult problems where higher derivatives may be discontinuous or boundary and interior layers occur. To analyze these problems a C^1 orthogonal collocation scheme on finite elements was devised and applied to a representative "effectiveness factor" problem with a boundary-layer [6]. Problems such as these are best handled by discrete element methods, particularly if used in conjunction with an adaptive refinement algorithm that can grade the mesh appropriately into the layers.

The solid phase consists of a porous base material impregnated with a catalytic material. Typically, the geometry consists of slabs, cylindrical rods or spherical pellets. For these simple geometrical configurations the governing equation simplifies to a nonlinear ordinary differential equation. In particular, a first order, irreversible, non-isothermal reaction in the catalyst material may be described by

$$\frac{1}{x^{a-1}}\left(x^{a-1}u'\right)' = f(x,u), \qquad 0 < x < 1 \tag{18}$$

where $a = 1, 2,$ or 3 is the dimension and boundary conditions are $u'(0) = 0$ and, for example, $-u'(1) = B(u(1) - 1)$, parameter B. For $f = \phi^2 u \exp\{\gamma(1-1/T)\}$ $T = 1 + \beta\delta + \beta(1 - \delta)u(1) - \beta u(x)$ and reaction rate parameters $\phi = 14.4$, $\beta = 0.02$, $\gamma = 20.0$, $\delta = 50$, $B = 250$, the problem has multiple solutions, the one of interest possessing a boundary-layer profile of order 10^{-3} near $x = 1$.

As the Thiele modulus ϕ increases towards 14.4, successive iteration on the nonlinear term becomes ineffective. Newton iteration is successful in determining the boundary-layer solution of practical interest. The Jacobian matrix is easily evaluated as the nonlinear term contributes only to the diagonal entries and to the last column. The general sequence of computations is depicted in the flowchart of Figure 2, [2].

[Figure 2]

Applying the refinement algorithm to this problem, we again initiate solution with a coarse mesh of four elements. Results for three refinement-iteration experiments are presented in Figure 3. The parameters C_1, C_2 are the residual tolerances in the stopping condition for successive Newton iterates. The graph demonstrates that a single Newton iteration per mesh is most efficient for this problem.

Even if the "final" graded mesh is employed directly with the same starting guess, more operations (1.64×10^6) are required than in the adaptive refinement solution (1.25×10^6). Moreover, in general we do not have sufficient advance knowledge of the solution behavior to affix such a severely graded mesh.

[Figure 3]

7. Potential Flows

A class of linear and nonlinear flow problems that are of considerable

practical importance in aerodynamics arise in potential flow theory. We begin with a treatment of mesh refinement applied to incompressible potential flow. In particular, the local approximation near the leading edge of a 10 percent biconvex airfoil is examined. The class of problems is then enlarged to admit compressible flows, the nonlinearity entering through the density. Here a practical problem of current interest is transonic airfoil design. The objective is to devise techniques and efficient algorithms for the transonic flow regime. We select this class of flows as representative nonlinear applications for refinement studies. The theory and strategies are directly applicable to other nonlinear problems as indicated in the previous sections and the brief discussions of other flow examples in the concluding sections of this paper.

8. Incompressible Flow

Conservation of mass together with irrotationality lead to the standard potential equation for incompressible two-dimensional steady flows, $\Delta \Phi = 0$ in Ω. In this instance, let us examine uniform flow about a 10 percent biconvex airfoil at zero angle of attack.

The potential function for the fully-infinite exterior flow field may be determined from classical complex variable theory [7],

$$\Phi(x,y) = \frac{\sinh b \cosh b}{\frac{n}{2} \{(\sin a \cosh b)^2 + (\cos a \sinh b)^2\}} \tag{19}$$

where

$$a = \frac{1}{n} \left(\tan^{-1} \frac{y}{x-1} - \tan^{-1} \frac{y}{x+1} \right)$$

$$b = \frac{1}{n} \ln \left[\{(x+1)^2 + y^2\}^{\frac{1}{2}} / \{(x-1)^2 + y^2\}^{\frac{1}{2}} \right]$$

and $\quad n = \frac{2}{\pi} \cos^{-1} \{(1-\delta^2)/(1+\delta)^2\}$, $\quad$ camber δ .

There is a stagnation point at the leading edge and the solution is less smooth in this neighborhood. Similar problems arise in other applications involving corners or cracks, and local mesh refinement becomes important. In general, for the Laplacian on a domain Ω with corner angle $\alpha\pi$, the leading term in the singularity of ϕ at the corner has the form $r^{1/\alpha}\sin\theta/\alpha$. When $\alpha > 1$ the corner is not convex and the first derivatives of ϕ are unbounded. In the present instance, since the flow field is symmetric the corner angle $\alpha\pi$ is less than π so that the potential and velocity components (first derivatives of Φ) are well behaved here. The magnitude of the velocity q decreases to zero at the stagnation point and then increases to a maximum at the topmost point of the airfoil. In general, there are fewer than $1/\alpha$ derivatives at the stagnation point and $1 + 1/\alpha$ derivatives in a mean-square sense. For $1/2 \leq \alpha < 1$ there are only two derivatives in a mean-square sense so the solution $\Phi(x,y)$ is in H^2. If the airfoil is at a small angle of attack the symmetry condition cannot be applied so that $1 \leq \alpha < 2$ and the solution is only in H^1. In the nonlinear problem to follow, we are no longer dealing with Hilbert spaces and, moreover, the nature of the singularity and space are not known.

In the following numerical experiment we examine the merit of refining locally in a subregion near the stagnation point. The effect of this strategy for nonlinear analysis of compressible and transonic flows is then considered.

As the flow field is symmetric, it is sufficient to consider a single quadrant. The complex variable solution is utilized to provided Dirichlet data in the far field on a remote but finite boundary - the first "window" in a sense. Our mesh of triangular elements is generated automatically in the region, as depicted in Figure 4. Here the principles of conformal mapping are introduced: we identify a map between a reference "rectangular" domain and the actual flow region. The mapping is defined by solving the Dirichlet

problems for the Laplacian, $\nabla^2 x = 0$ and $\nabla^2 y = 0$, on the $(\hat{x}, \hat{y})$ reference region. Finite element techniques are well-suited to this task and the same program can be used as in the flow computations. The nodal solution vectors of coordinate values $\{x_i\}, \{y_i\}$ at nodes $\{i\}$ in $\hat{\Omega}$ define the nodal locations in Ω [8].

This data basis and the generated data set are used repeatedly with very minor modifications for successively refined subregions. Two further refinements termed Mesh 2 and Mesh 3 are made in each of the computations for this flow problem. The corresponding subregions are marked in the figure.

[Figure 4]

8.1 Results

A finite element approximation $\tilde{\phi}(x,y)$ to the potential field is calculated using the given mesh of linear elements, Mesh 1. This approximation, the exact solution, and error at representative points on the airfoil are listed in Table 1, and compared there with corresponding values obtained using Mesh 2.

Contour lines for the relative error $e(x,y) = \{\phi(x,y) - \tilde{\phi}(x,y)\}/\phi(x,y)\}$ are graphed in Figure 5. The contour levels range from 0.0 in the far field to .0144 at approximately the 1/6 chord position on the airfoil. As anticipated, the contours are widely separated away from the obstacle and dense in the near field where the error function rises abruptly towards the airfoil. The subdomain Ω_2 for Mesh 2 is superimposed on the plot. The root-mean-square (RMS) error on Ω_1 for Mesh 1 gives $\ln(\overline{E}_{1,-1}) = -5.7$ for N = 63 node points. On the subregion Ω_2 the error for this mesh has $\ln(\overline{E}_{2,1}) = -5.2$ for N = 25 and for $(\overline{E}_{3,1}) = -4.8$ for N = 7.

Subregion Ω_2 is next considered and the same mapping approach utilized to generate Mesh 2. The boundary data is interpolated from the previous finite element solution on Mesh 1. As part of the investigation, both exact and prior finite element solutions were used to provide boundary data on Ω_2.

The results are consistent with those predicted from the theory earlier (following equation (15)). The question of error propagation from a boundary is more interesting and difficult for the nonlinear transonic problem. Disturbances in the supersonic flow will propagate essentially unchanged along characteristics whereas a maximum principle holds here for the linear problem.

Solution and error values at surface nodes for finite element computations on Mesh 2 are given in Table 1. Again, the error contour levels have the same qualitative character as obtained using Mesh 1 on Ω_1 in Figure 6. However, they are now less densely clustered and range from 0.0 in the "new" far-field to .007 at approximately the 1/6 chord position on the airfoil. The error is markedly reduced from that of the previous calculation: the log of the RMS error on Ω_2 with Mesh 2 is $\ln(\overline{E}_{2,2}) = -6.2$ for N = 63 node points. Following the previous procedure, we identify the subregion Ω_3 and compute $\ln(\overline{E}_{3,2}) = -6.0$ for N = 17. The actual choice of Ω_3 is more appropriately suited to the nonlinear problem. As we shall see in the next section the nonlinear compressibility effects are most important near the leading edge.

The final solution on Mesh 3 with boundary data from Mesh 2 produces a similar error contour plot. The log of the RMS error on Ω_3 is $\ln(\overline{E}_{3,3}) = -6.35$ for N = 63. The error at the stagnation pont is .0015. The numerical experiments and results are described in greater detail in reference [9].

[Figures 5-6, Table 1]

9. Compressible and Transonic Flow

The development of the nonlinear compressible flow field about an airfoil is now examined. Let M_∞ denote the uniform upstream Mach number in the far field. An appropriate high Reynolds' number Re is assumed so that the flow remains attached well beyond the critical Mach number M_c. For M_∞ slightly greater than M_c, local supersonic pockets form on the upper and lower surfaces of the airfoil. Supersonic Mach numbers in the pockets are

near unity and there is no distinguishable steady shock. As M_∞ increases further, a steady shock appears at the rear boundary of the supersonic pocket. This occurs when M_{max} is approximately 1.05. If M_∞ continues to increase, the supersonic region grows and the shock moves downstream, increasing in strength. A pressure jump occurs across the shock, and this eventually at some M_∞ will lead to boundary-layer separation.

Finite element computations of compressible subsonic and slightly super-critical flows are next carried out in conjunction with "windowing" for mesh refinement. We repeat the sequence of computations on the meshes described in the previous section for incompressible aerodynamic flows. For transonic flows the problem is of mixed type, being elliptic in the subsonic region and hyperbolic in the supersonic pocket. The mixed flow type, nonlinearity and shock discontinuities are primary areas of difficulty. We shall consider only the first two of these in this investigation. In particular, accurate and efficient nonlinear solutions are sought in the vicinity of the airfoil. The exact solution is now unknown, and we are unable to examine errors explicitly as we did in the previous linear problems.

The finite element formulation is first summarized. Using the Bernoulli relation together with the adiabatic equation of state in the continuity equation, we have the transonic full potential equation [9]

$$\{1 + M_\infty^2 \frac{(\gamma-1)}{2}(1 - \phi,_j^2)\}\phi,_{ii} - M_\infty^2\phi,_i\phi,_j\phi,_{ij} = 0 \tag{20}$$

where M_∞ is the Mach number of the uniform remote flow and Cartesian tensor notation has been employed.

Equivalently, we may rewrite the equation in the form

$$(a^2 - \phi_x^2)\phi_{xx} - 2\phi_x\phi_y\phi_{xy} + (a^2 - \phi_y^2)\phi_{yy} = 0 \tag{21}$$

where $a^2 = a_\infty^2 + \frac{(\gamma-1)}{2} (U_\infty^2 - \phi_x^2 - \phi_y^2)$ defines the local speed of sound, γ is the gas constant, and U_∞ is the uniform remote flow. The associated boundary conditions in the far field are

$$\Phi \to U_\infty x \quad \text{as} \quad x^2 + y^2 \to \infty$$

and on the airfoil $\phi_y/\phi_x = f_x$ where $f(x,y)$ describes the upper surface.

A corresponding variational problem suitable for finite element computations can be constructed. The functional is

$$I = \int_A \{1 + \frac{\gamma-1}{2} M_\infty^2 (1 - \phi_{,i}^2)\}^{\gamma/\gamma-1} \, dA \tag{22}$$

Introducing a linear finite element approximant into the integrand and carrying out the usual variational procedures yields the element contribution to the nonlinear finite element system

$$\frac{\partial I_e}{\partial \phi_e} = A_e \left\{ 1 + (\frac{\gamma-1}{2})M_\infty^2(1 - \phi^T M \phi) \right\}_e^{\frac{1}{\gamma-1}} M_e \phi_e \tag{23}$$

where A_e is the element area and $M_e = L_x L_x^T + L_y L_y^T$ with $\Phi_e(x,y) = L^T \phi_e$.

This formulation and other approximate analyses are treated in greater detail in reference [9]. We consider mesh refinement and numerical solution of the nonlinear equations $g(\phi) = 0$ obtained from equation (23). Element contributions to the Jacobian matrix in a Newton-Raphson iterative procedure can be derived directly from (23). That is, $J(\phi^{(i+1)} - \phi^{(i)}) = -g^{(i)}$ for iterate $i+1$, and for each element

$$J_e = A_e \{\beta^{\frac{1}{\gamma-1}} M_e + (\gamma-1)M_\infty^2 \beta^{\frac{2-\gamma}{\gamma-1}} (M\phi)_e (M\phi)_e^T \} \tag{24}$$

where $\beta = [1 + \frac{(\gamma-1)}{2} M_\infty^2 (1 - \phi^T M \phi)]_e$.

In the following numerical experiments Newton-iterative solution is combined with mesh refinement on successive windows adjacent to the leading edge.

9.1 Results

Nonlinear finite element analysis with the nested meshes of Figure 4 is now examined for compressible flow about the biconvex airfoil. Solutions are computed at a subcritical incident Mach number $M_\infty = 0.6$ and at the slightly supercritical Mach number $M_\infty = 0.795$. Isomach contours are graphed in Figure 7 for the subcritical flow ($M_\infty = 0.6$) on Ω_1 using Mesh 1.

[Figure 7]

In the numerical experiments we combine refinement of subregions with Newton iteration to a variable tolerance (error level). For example, the finite element solution on Mesh 1 is computed to a tolerance $\tau = 10^{-2}$ in the Newton iteration. This requires 6 Newton iterates from the incompressible starting solution. The solution is then sought on Ω_2 with Mesh 2 and to a tolerance of $\tau = 10^{-3}$ in successive Newton iterates. Finally, using the solution from Mesh 2, iteration proceeds on subdomain Ω_3 and Mesh 3 at tolerance $\tau = 10^{-4}$.

The behavior of the error in successive Newton iterates is analogous to that of the error function in the linear potential problems treated earlier. In Figure 8 contours of solution iterate error on Mesh 1 are graphed. Contour values range from -.006 to zero. The log of the RMS iterate error is -6.4 for N = 63. Continuing to Mesh 2 on Ω_2 at tolerance 10^{-3} the error contours range from -2.6×10^{-4} to 1.4×10^{-4} and $\ln(\overline{e}_2) = -14.4$ after 2 iterations. Values of $\tilde{\Phi}$ and iterate error $|e|$ at points on the airfoil surface are given in Table 2. Finally, on Ω_3 with Mesh 3 and a starting iterate interpolated from the current iterate on Mesh 2, at $\tau = 10^{-4}$ the contours range from -8.1×10^{-7} to 5.4×10^{-7} and are shown in Figure 9. The

log of the RMS iterate error is -14.0 after 3 Newton iterations.

The important point is that the absolute errors in each solution iterate are near zero away from the airfoil and increase to a maximum near the leading edge. Again, we are exploiting this feature of the error behavior, but in this instance as applied to iteration errors rather than the solution error. Rapid convergence in the far field allows us to reduce the domain and use the previous "coarse mesh solution" to interpolate an excellent starting guess on the new, finer mesh in the near field.

We do not mean to infer that the actual error has the same behavior. In fact, we know that the iterate error at the boundary is no better than that of the previous mesh. Yet, it may be argued that, *relative to this error*, the errors in the interior of following subregions are being reduced to zero. The final result is a solution in the neighborhood of interest, the near field of the airfoil, and on a fine mesh that is of satisfactory accuracy. Furthermore, this nonlinear solution has been obtained very efficiently.

[Figures 8-9, Table 2]

As we remarked earlier, the strategy proves useful if the successive boundaries remain in the subsonic flow. The refinement approach is also successful for supercritical flows. At $M_\infty = .8$ there is a small supersonic pocket adjacent to the topmost part of the airfoil. On Mesh 1 we find a single element of the coarse mesh is supersonic. Progressing to Mesh 2, there are several smaller elements that are supersonic and we obtain much better resolution of the sonic line and mixed flow.

To achieve convergence of the Newton iteration at supercritical Mach numbers, we require an accurate starting iterate on an appropriate mesh. In the present case, for mildly transonic flows accurate computations of

the flow field near the leading edge can be obtained as follows: (1) Begin
with an initial mesh on the largest domain and compute a potential solution;
(2) Using the same mesh work up in Mach number and with few Newton iterates
until the dominant changes in the solution are localized near the airfoil;
(3) Introduce the new mesh, interpolating nodal solutions from the most re-
cently calculated vector on the previous mesh; (4) Continue iteration at
this Mach number on the new subregion and on following subregions.

If accurate approximations at the higher Mach numbers cannot be attained
on the initial mesh then errors at newly-introduced boundaries may lead to
difficulties. Alternative iterative methods such as point relaxation schemes
may be applied to make the basic system solution more robust. These are cur-
rently being investigated [8].

10. Other Problems and Refinement Techniques

In this final section a brief overview of other techniques and
applications is presented. Within this more general context one can
examine competitive refinement, enrichment, mesh equidistribution and
subregion refinement strategies and the classes of applications to which
they are best suited. Directions of continuing research in refinement
theory and technique are described. In particular, the implications
of these techniques to time-dependent problems and some related pro-
blems peculiar to refinement are noteworthy.

10.1. Refinement Techniques

Mesh refinement in one dimension is relatively straightforward.
The techniques described earlier for mesh enrichment guided by the

residual are qualitatively similar to utilizing the truncation error in finite difference formulations. An alternative approach, termed "equi-distribution" in the finite difference literature, cons ers a mesh of grid points and redistributes the mesh according to an error criterion such as the residuals developed here. A simple strategy is "doubling and halving" whereby the mesh size h is doubled in regions where the solution is better behaved and existing elements halved in elements where refinement is desired. Other "monitor" functions such as arc length and measured of the local rate of change of solution have been applied, particularly in finite difference and finite element colloca-tion computations. A survey and bibliography is forthcoming [11]. One may also refine by increasing the order of the element, a relatively easy process in one dimension but obviously sensitive to the quality of the initial mesh.

Refinement in two or three dimensions is more difficult. Elements meet along edges and surfaces respectively and refinement will often introduce new nodes on the boundary of the original element. One or two internal refinements that do not introduce any new nodes on the old boundary might be acceptable. Engineering experience has shown that idealizations with slender elements may often yield poor results. Mathematically, we require that the finite element basis should be *uniform*. This amounts to a constraint on the element geometry. If the finite element approximation U(x,y) coincides with the exact solution at the nodes of a triangular element, then

$$\left| \frac{\partial u}{\partial x_i} - \frac{\partial U}{\partial x_i} \right| \leq \frac{1}{2} \frac{Kd}{\sin \theta} \tag{25}$$

where K is a bound on $|\partial^2 U/\partial x_i \partial x_j|$, d is the diameter of the element and θ is the largest angle of the triangle. The need for caution is evident from the dependence of the bound on angle θ . Also, slender triangles may lead to deterioration of the numerical condition of the algebraic system.

The natural refinement of a three-node triangle is to introduce new nodes at the side mid-points and subdivide the triangle into four congruent subtriangles. Additional midside nodes are shared with adjacent elements. Across an interface between refined and unrefined regions the approximation must be constrained to ensure continuity. The constraint can be embedded directly in the basis, and the approach has been used successfully for refinement towards a singular point [12]. Alternatively, Lagrange multipliers may be introduced to satisfy the continuity requirement on the interface S between refined and unrefined regions. For potential flows the variational problem becomes:

make stationary the functional

$$I = \int_{\Omega} \frac{1}{2}(\phi_x^2 + \phi_y^2)d\Omega + \int_S \lambda(x,y)(\Phi_+ - \Phi_-)ds \qquad (26)$$

where Φ_+ and Φ_- represent the approximations in the refined and unrefined subregions adjacent to S . The argument can be applied using penalty constraints rather than multipliers in the usual manner and utilised in nonlinear problems such as the compressible flow examples considered earlier. In fact, for the transonic small disturbance equation [9] the modified functional is very similar to that above,

$$I_1 = \int_\Omega (\frac{K}{2} - \frac{1}{6} \Phi_x^3 + \frac{1}{2} \Phi_y^2) d\Omega$$

$$+ \int_S \lambda(x,y)(\Phi_+ - \Phi_-) ds \qquad (27)$$

An approximate analysis requires finite element expansions for both $\Phi(x,y)$ in Ω and $\lambda(x,y)$ on S slightly increasing the size of the algebraic problem. Details of the formulation and implementation are described elsewhere [13].

For many applications, excluding solutions possessing layers and singularities, only moderate refinement is required. In this event the additional complexity arising from the imposed constraint on exposed nodes may be avoided by alternative refinements. One scheme, that has been utilized in an algorithm for linear and nonlinar problems, is to bisect the largest angle of a triangle and continue by subdividing the adjacent element on the newly divided side [14]. The largest angle of the second triangle may not be bisected so that some slender elements may develop. Yet for many applications it is unlikely that there would be extensive bisections of a small angle early in the

refinement process. In [14] this approach is applied to $\Delta u = 1/4 \, u^3/r^3$ in a triangular domain with $\partial u/\partial n + u^4 - r^2 = 0$ on the slant side and $u = \sqrt{r}$ (the solution) on the remainder of the boundary. Refinement proceeds from an initial triangulation of 3 elements to 60 elements after 7 steps. The maximum error is 3.6×10^{-4}.

The approach of refining nested subregions that is used in the potential flow experiments of earlier sections has been in use at least since the mid-sixties in finite difference computations and

probably was practised much earlier than this. In industrial research applications it has been in use in finite element computations since the late sixties and, applications to fluid mechanics problems have been made recently [15,16]. In [15] the method is applied to viscous flow through a two-dimensional diverging channel. The Reynolds number of the flow is increased until primary vortices appear. In this particular application the separation region in the channel is studied in detail by re-meshing on the pertinent subregion. Oscillatory behavior of the solution at moderate Reynolds numbers (around 37.5) necessitate the use of under-relaxation methods. A similar point arises in the analysis of supercritical compressible flows, but the behavior of the iteration improves on successive nested meshes. Elsewhere [16] the incompressible viscous flow problem has been studied numerically using a primitive variable formulation with nested refined subregions. It is observed from experiments that the procedure again is suitable for detailed examination of separation with closed recirculation regions. As in the case of the supersonic pocket studies, details of the flow near the point of interest are not evident on the coarse mesh solution but are resolved on subregion refinement. For a rectangular subregion the velocity boundary data may be interpolated on three sides from the previous coarse-mesh solution. On the remaining side numerical experiments indicate that the pressure distribution is required to ensure that mass is conserved in the subregion. If velocity is also specified on the fourth-side numerical instabilities arise as the incompressibility condition is satisfied only in an integral sense on the subregion. Detailed numerical results are obtained for corner recirculation in a driven cavity flow at Reynolds number 100.

Recent theoretical work in the form of the residual analysis [2, 16] is establishing a theoretical foundation for existing and future refinement strategies in finite element computations and there are many challenging problems in all areas of analysis, algorithm and implementation. These difficulties notwithstanding, in closing, we raise the issue of time-dependent analysis and adaptive refinement. Equidistribution techniques such as the "doubling and halving" strategy are being applied to wave propagation problems. Consider a propagating step-front, a model problem frequently studied of convection-diffusion processes. A fine mesh is desired in the vicinity of the propagating front. A strategy currently being explored utilizes a residual analysis within a semi-discrete finite element formulation, enriching the spatial mesh at times and locations determined by the error criterion.

11. Concluding Remarks

An eventual goal might be to formulate and implement a theory for adaptive refinement whereby the analyst may specify conditions such as desired global or local accuracy, processing cost, or storage limitations, to determine an appropriate mesh. Realistically, when one deals with general linear and nonlinear problems this ideal can not be attained - the degree of difficulty of the problems and their diversity is too severe. As we have demonstrated, substantial progress can be made if one restricts the strategies to specific classes of problems - here certain linear and nonlinear flow and transport problems.

Even if the more ambitious general goal is ignored, one can apply refinement analysis and algorithms to great advantage. This is particularly true if the problems considered have layers or singularities, especially if their location is not well known in advance. In treating nonlinear problems, much of the underlying computation required to generate an accurate solution

iterate and also an appropriate mesh, can be carried out economically on coarse meshes. The nonlinear iteration and adaptive mesh refinement can thus be interwoven to produce efficient algorithms.

Acknowledgements

References

1. Oden, J. T. and J. N. Reddy: Mathematical Foundations of the Finite Element Method, Wiley Interscience, 1977.

2. Humphrey, D. and G. F. Carey: "Adaptive Mesh Refinement Algorithm Using Element Residuals," TICOM Report 78-1, Texas Institute for Computational Mechanics, University of Texas at Austin, 1978.

3. Guerra, F. and E. B. Becker: "Finite Element Analysis for the Adaptive Method of Rezoning," TICOM Report 78-7, Texas Institute for Computational Mechanics, University of Texas at Austin, 1978.

4. Babuska, I., W. Rheinboldt and C. Mesztenyi: "Self-adaptive Refinements in the Finite Element Method," Tech. Rept. TR-75, Inst. for Fluid Dynamics and Applied Mathematics, Univ. of Maryland, 1975.

5. Finlayson, B. A.: The Method of Weighted Residuals and Variational Principles, Academic Press, 1972.

6. Carey, G. F. and B. A. Finlayson: "Orthogonal Collocation on Finite Elements," J. Chem. Eng. Science, Vol. 30, pp. 587-596, 1975.

7. Milne-Thompson, L. M.: Theoretical Hydrodynamics, 5th Edition, McMillan, New York, 1968.

8. Akin, E.: "Finite Element Analysis, Its Implementation and Application," TICOM Report 77-13, 1977.

9. Carey, G. F. and T. T. Pan: "Studies in Computational Transonics I," TICOM report (in preparation), 1978.

10. Carey, G. F.: "Computational Transonics," Chapter 9 of Finite Elements in Fluids, Vol. 3, R. H. Gallagher et al (eds.) John Wiley and Sons, 1979 (in press).

11. Russell, R.D.: "Survey paper on Mesh Refinement for Two-Point Problems," to appear in Lecture Notes in Computation, Springer-Verlag, 1978 (in press).

12. Carey, G.F.: "A Mesh-Refinement Scheme for Finite Element Computations," Jnl. Comp. Meth. in Applied Mechanics and Eng., Vol. 7. No. 1, pp. 93-105, Jan. 1976.

13. Carey, G.F.: "Finite Element Meshes, "TICOM report (in preparation), TICOM, Univesity of Texas at Austin, 1978.

14. Sewell, G: "An Adaptive Computer Program" in MAFELAP 1975, ed. J. Whiteman, Academic Press, London, pp. 125-144, 1976.

15. deVries, G., R. Balasubramanian and D.H. Norrie: "The Application of the Pseudo-Functional Finite Element Method to Viscous Flow Problems," M.E. dept. report No. 63, U. Calgary, May 1974.

16. Gartling, D.K. and E.B. Becker: "Finite Element Analysis of Viscous Incompressible Fluid Flow," Parts I and II, Jnl. Comp. Meth. in Applied Mech. and Eng., Vol. 8, No. 2, pp. 51-60 and pp. 127-138, 1976.

17. Babuska, I. and W.C. Rheinboldt: "On the Reliability and Optimality of the Finite Element Method," U. Maryland Tech. Rept. TR-643, April 1978.

List of Figures

List of Tables

Table 1

Surface Nodes		Mesh 1			Mesh 2	
x	y	Φ	$\tilde{\Phi}$	E	$\tilde{\Phi}$	E
.473	.078	.5289	.5214	.014	.525	.008
.747	.044	.8239	.8117	.015	.8196	.005
.907	.018	.9845	.9713	.013	.9792	.005
1.000	.000	1.068	1.060	.008	1.065	.003

Solution and error values at representative nodal points in successive meshes.

Table 2

Surface Nodes		Mesh 1		Mesh 2	
x	y	$\tilde{\Phi}$	$|e|$	$\tilde{\Phi}$	$|e|$
.473	.078	.5376	.001	.5479	10^{-6}
.747	.044	.8327	.007	.8408	10^{-6}
.907	.018	.9915	.006	.9960	10^{-6}
1.000	.000	1.0778	.005	1.078	10^{-6}

Newton iterate error behavior on subdomain Ω_3 for successive meshes
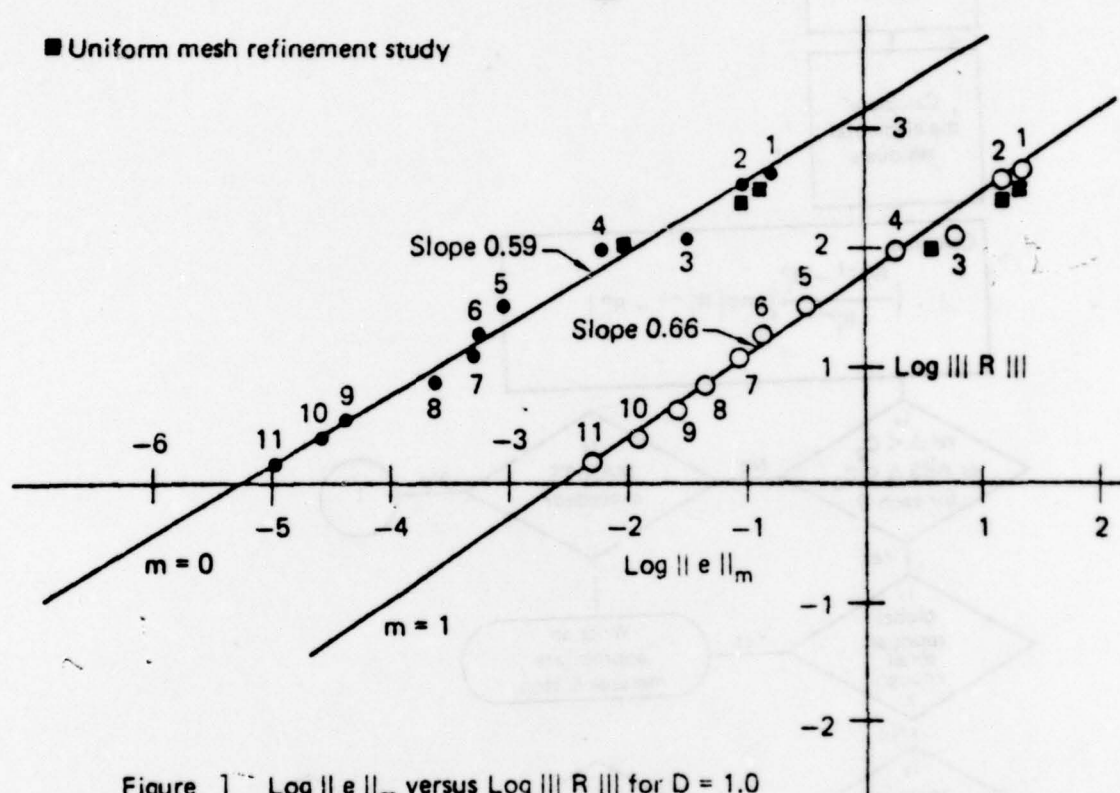
Figure 1 Log $\|e\|_m$ versus Log $\|\|R\|\|$ for D = 1.0
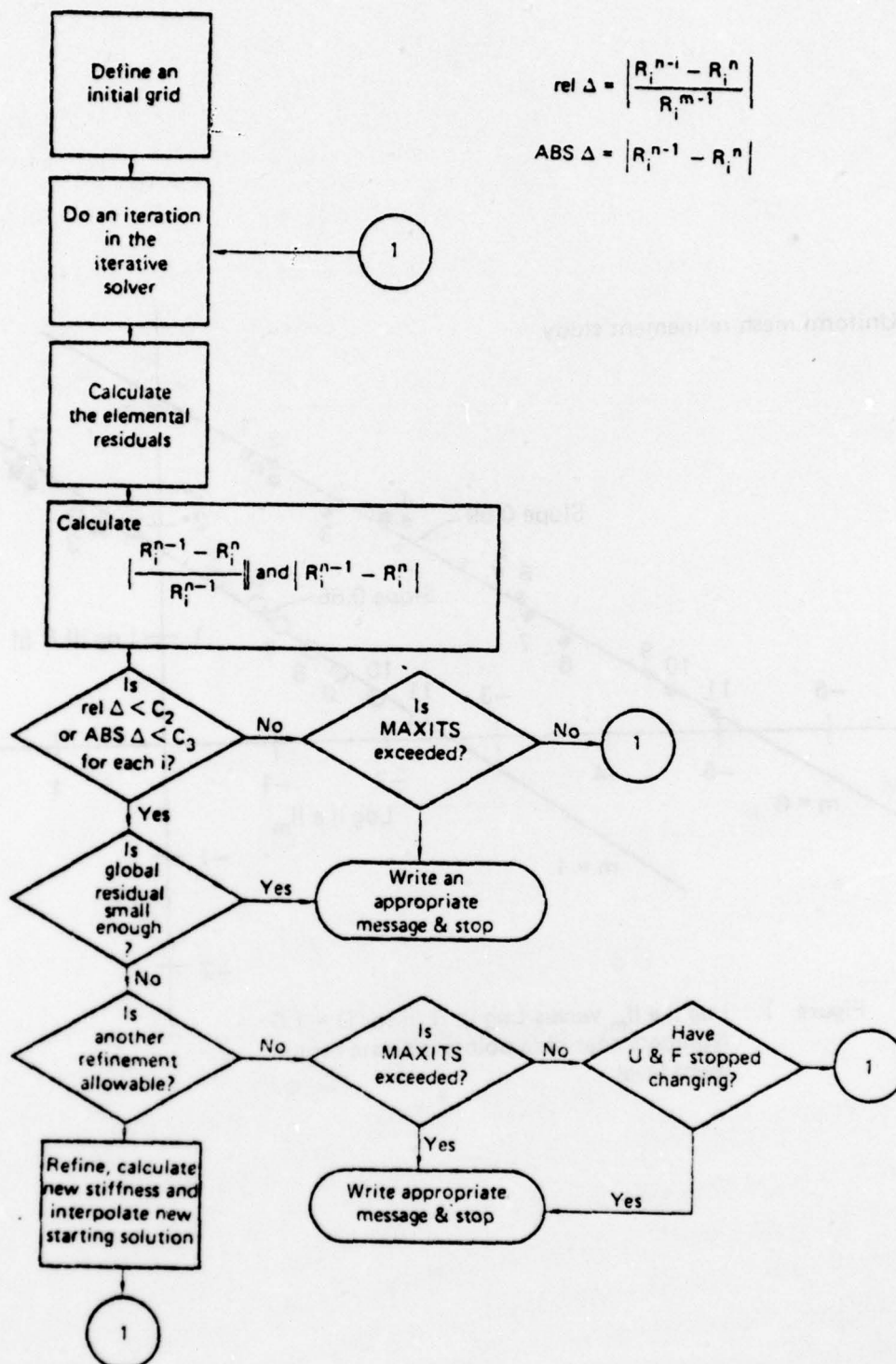Numbers near data points indicate refine-
ment level.

Define an
initial grid

Do an iteration
in the
iterative
solver

1

Calculate
the elemental
residuals

Calculate

$$\left|\frac{R_i^{n-1} - R_i^n}{R_i^{n-1}}\right| \text{ and } \left|R_i^{n-1} - R_i^n\right|$$

Is
rel $\Delta < C_2$
or ABS $\Delta < C_3$
for each i?

No — Is MAXITS exceeded? — No — 1

Yes

Is
global
residual
small
enough
?

Yes — Write an appropriate message & stop

No

Is
another
refinement
allowable?

No — Is MAXITS exceeded? — No — Have U & F stopped changing? — 1

Yes — Write appropriate message & stop — Yes

Refine, calculate
new stiffness and
interpolate new
starting solution

1

$$\text{rel } \Delta = \left|\frac{R_i^{n-1} - R_i^n}{R_i^{m-1}}\right|$$

$$\text{ABS } \Delta = \left|R_i^{n-1} - R_i^n\right|$$

Figure 2 Flowchart of refinement process for nonlinear problems.
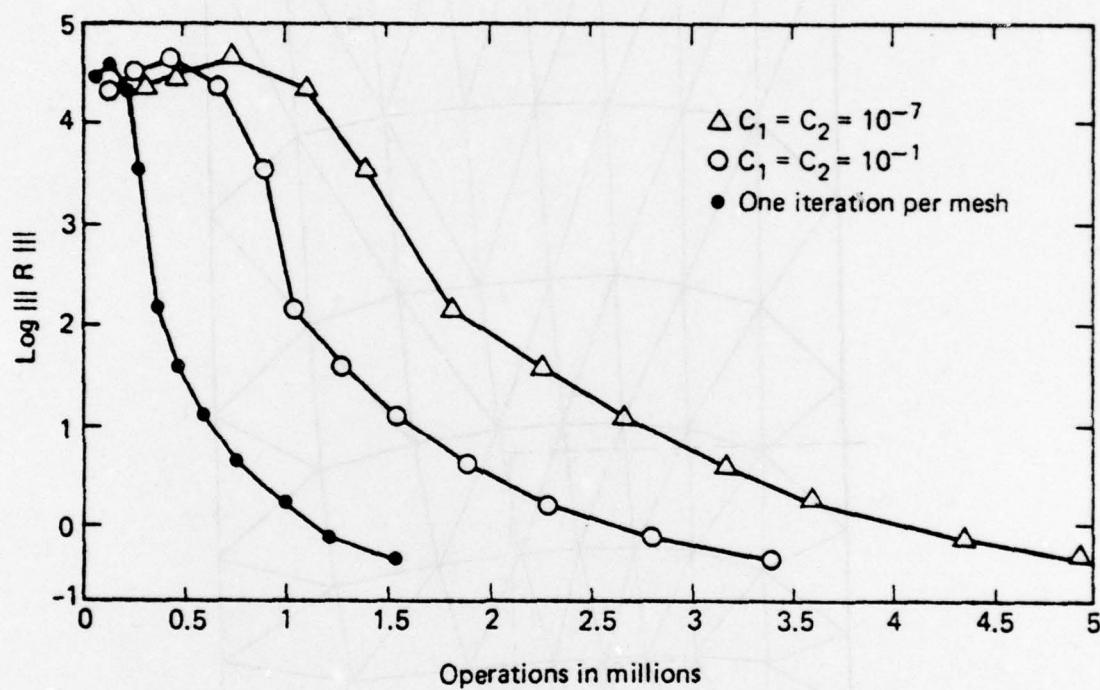
Figure 3   Operation counts versus global residual for D = 1.0.
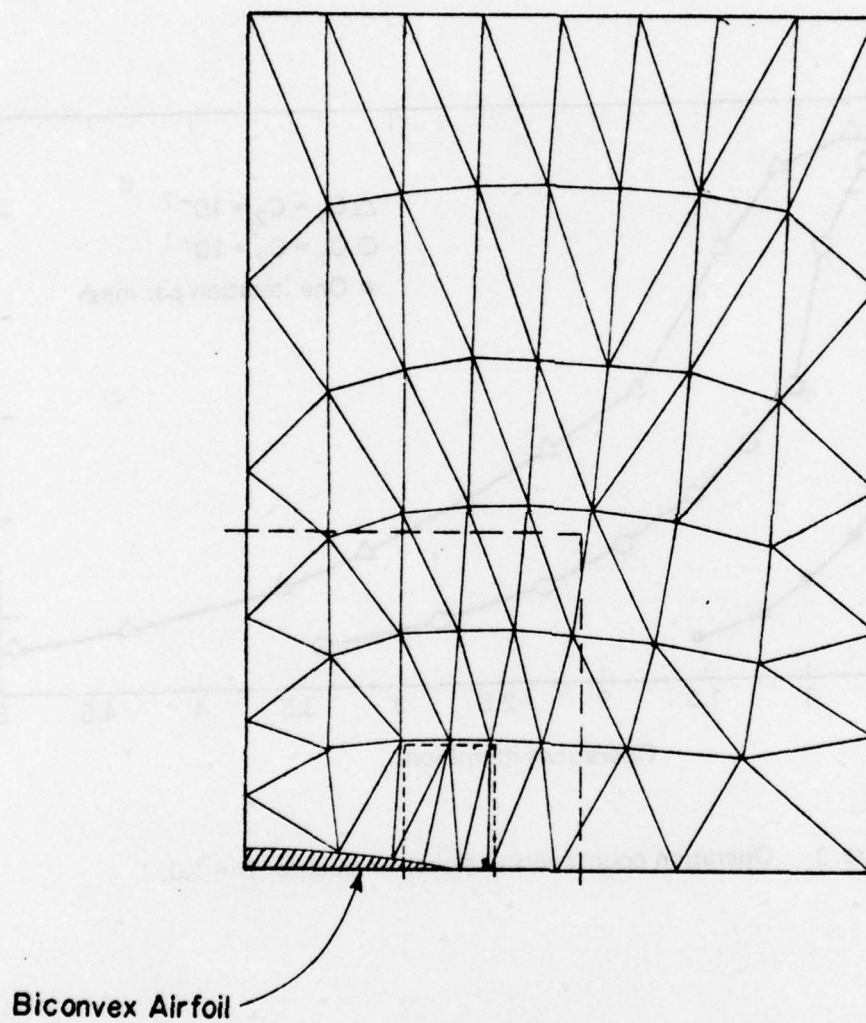
Biconvex Airfoil

Figure 4. Grid generation by mapping between reference and physical planes. Successive subregions for refinement are marked.

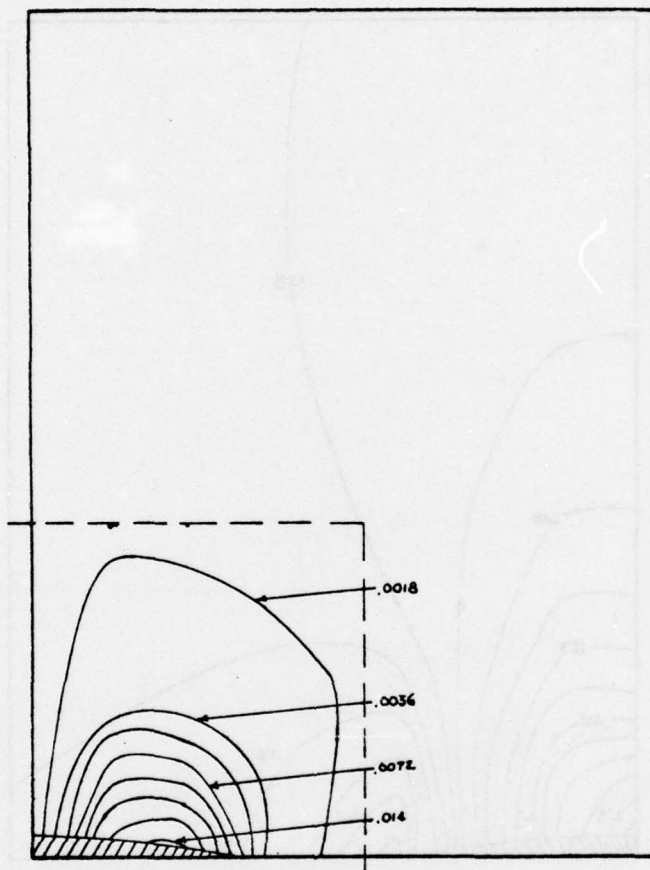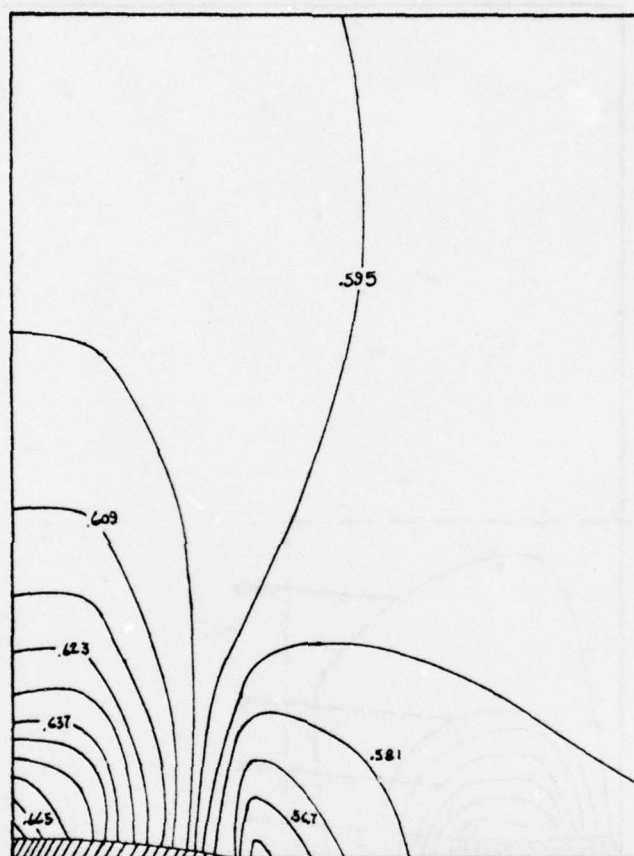Figure 5. Error contours for original domain Ω_1 and Mesh 1.

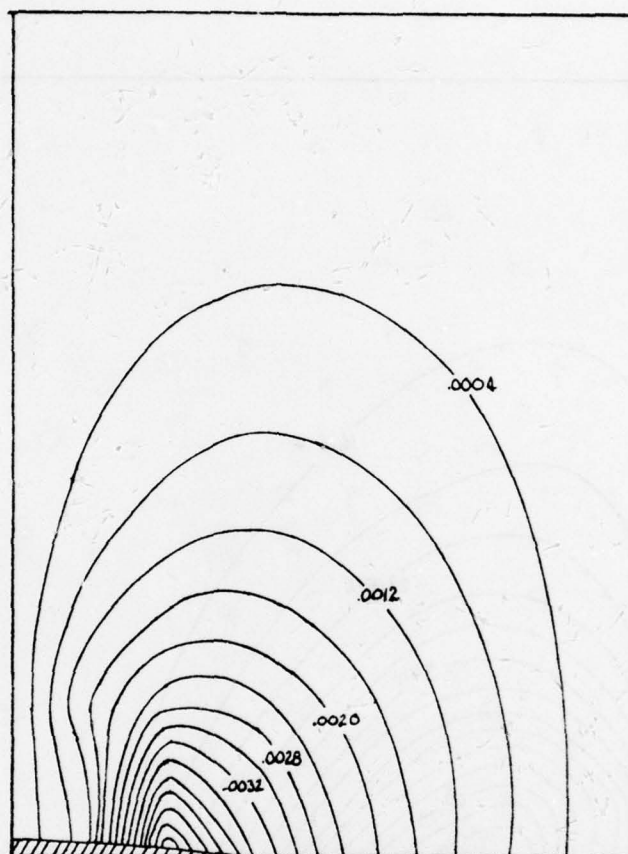Figure 6.   Error contours for final subregion Ω_2 and Mesh 2.

Figure 7. Compressible flow solution: Mach line
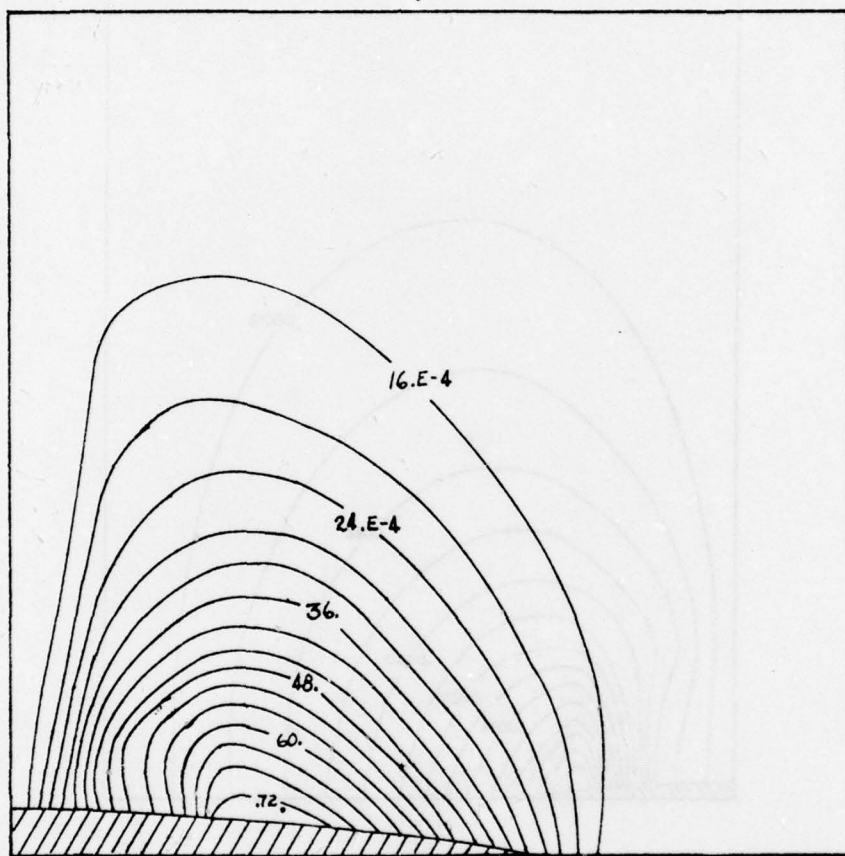contours for incident flow at M_∞ = 0.6
on Mesh 1.

Figure 8. Contours of iterate error on Mesh 1 at $M_\infty = 0.6$, $\tau = 10^{-2}$.
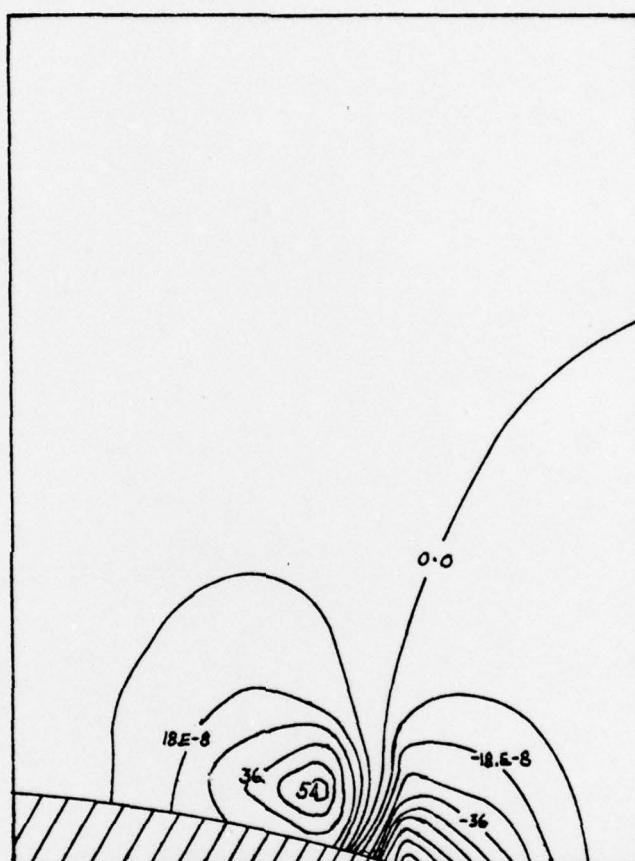
Figure 9. Contours of iterate error on Mesh 3 at $M_\infty = 0.6$, $\tau = 10^{-4}$.

REPORT DOCUMENTATION PAGE		READ INSTRUCTIONS BEFORE COMPLETING FORM
1. REPORT NUMBER TR-1	2. GOVT ACCESSION NO.	3. RECIPIENT'S CATALOG NUMBER
4. TITLE *(and Subtitle)* Adaptive Refinement and Nonlinear Fluid Problems		5. TYPE OF REPORT & PERIOD COVERED Technical Report
		6. PERFORMING ORG. REPORT NUMBER TR-1
7. AUTHOR(s) G. F. Carey		8. CONTRACT OR GRANT NUMBER(s) N00014-78-C-0550
9. PERFORMING ORGANIZATION NAME AND ADDRESS Texas Institute for Computational Mechanics University of Texas at Austin Austin, Texas 78712		10. PROGRAM ELEMENT, PROJECT, TASK AREA & WORK UNIT NUMBERS NR 064-478
11. CONTROLLING OFFICE NAME AND ADDRESS Office of Naval Research Arlington, Virginia 22217		12. REPORT DATE May 1979
		13. NUMBER OF PAGES 38
14. MONITORING AGENCY NAME & ADDRESS*(if different from Controlling Office)*		15. SECURITY CLASS. *(of this report)* Unclassified
		15a. DECLASSIFICATION/DOWNGRADING SCHEDULE

16. DISTRIBUTION STATEMENT *(of this Report)*

Unlimited

17. DISTRIBUTION STATEMENT *(of the abstract entered in Block 20, if different from Report)*

18. SUPPLEMENTARY NOTES

19. KEY WORDS *(Continue on reverse side if necessary and identify by block number)*

finite elements, meshes, adaptive refinement, mechanics, flows, nonlinear iteration

20. ABSTRACT *(Continue on reverse side if necessary and identify by block number)*

The research activity deals with theory and implementation of adaptive mesh refinement for finite element analysis of linear and nonlinear problems in mechanics. The theoretical ideas are based upon the use of residuals from the equilibrium equation and associated error bounds which relate the error in the solution to these residuals. The techniques are equally applicable to finite element applications in fluid and solid mechanics. The strategy of interweaving Newton iteration and adaptive refinement appears particularly effective for the nonlinear problems examined.

DD ₁ FORM JAN 73 1473   EDITION OF 1 NOV 65 IS OBSOLETE
S/N 0102-014-6601 |

Unclassified